Psychiatry Research: Neuroimaging 332 (2023) 111633

Contents lists available at ScienceDirect

Psychiatry Research: Neuroimaging

journal homepage: www.elsevier.com/locate/psychresns

Relationship between function and structure in the visual cortex in healthy individuals and in patients with severe mental disorders

Nora Berz Slapø [a,*], Kjetil Nordbø Jørgensen [a,b], Torbjørn Elvsåshagen [a,c], Stener Nerland [a,d], Daniel Roelfs [a], Mathias Valstad [e], Clara M.F. Timpe [a,f], Geneviève Richard [a], Dani Beck [a,d], Linn Sofie Sæther [a], Maren C. Frogner Werner [a], Trine Vik Lagerberg [g], Ole A. Andreassen [a,g], Ingrid Melle [a], Ingrid Agartz [g,d,h], Lars T. Westlye [a,f], Torgeir Moberget [a,i], Erik G. Jönsson [a,h]

[a] NORMENT, Institute of Clinical Medicine, University of Oslo, Norway
[b] Department of Psychiatry, Telemark Hospital, Skien, Norway
[c] Department of Neurology, Oslo University Hospital, Norway
[d] Department of Psychiatric Research, Diakonhjemmet Hospital, Oslo, Norway
[e] Department of Mental Disorders, Norwegian Institute of Public Health, Norway
[f] Department of Psychology, University of Oslo, Norway
[g] NORMENT, Division of Mental Health and Addiction, Oslo University hospital, Norway
[h] Centre for Psychiatry Research, Department of Clinical Neuroscience, Karolinska Institutet & Stockholm Health Care Sciences, Stockholm Region, Stockholm, Sweden
[i] Department of Behavioral Sciences, Faculty of Health Sciences, Oslo Metropolitan University, OsloMet, Oslo, Norway

ARTICLE INFO

Keywords:
P100 amplitude
Cortical thickness
Cortical surface area
Structural magnetic resonance imaging
Function-structure relationship in the cortex
Schizophrenia spectrum disorders
Bipolar disorders

ABSTRACT

Patients with schizophrenia spectrum disorders (SCZ_{spect}) and bipolar disorders (BD) show impaired function in the primary visual cortex (V1), indicated by altered visual evoked potential (VEP). While the neural substrate for altered VEP in these patients remains elusive, altered V1 structure may play a role. One previous study found a positive relationship between the amplitude of the P100 component of the VEP and V1 surface area, but not V1 thickness, in a small sample of healthy individuals. Here, we aimed to replicate these findings in a larger healthy control (HC) sample ($n = 307$) and to examine the same relationship in patients with SCZ_{spect} ($n = 30$) or BD ($n = 45$). We also compared the mean P100 amplitude, V1 surface area and V1 thickness between controls and patients and found no significant group differences. In HC only, we found a significant positive P100-V1 surface area association, while there were no significant P100-V1 thickness relationships in HC, SCZ_{spect} or BD. Together, our results confirm previous findings of a positive P100-V1 surface area association in HC, whereas larger patient samples are needed to further clarify the function-structure relationship in V1 in SCZ_{spect} and BD.

1. Introduction

Schizophrenia spectrum disorders (SCZ_{spect}) and bipolar disorders (BD) are severe mental disorders with largely unknown pathophysiology (Birur et al., 2017; Grande et al., 2016; McGrath et al., 2008; Merikangas et al., 2011). Many different brain circuits are likely to be involved, affecting both higher-order cognitive functions (McCutcheon et al., 2023) and more basic sensory (Dondé et al., 2019) and motor (Pieters et al., 2022) processing. For instance, functional studies point towards the involvement of the visual cortex. Several electroencephalography (EEG) studies on how the brain processes specific stimuli (Luck, 2014) have reported reduced amplitude of the P100 component of the visual evoked potential (VEP) in SCZ_{spect} (Butler et al., 2007; Doniger et al., 2002; Foxe et al., 2001, 2005; Lalor et al., 2012; Yeap et al., 2008, 2006). Further, altered VEP plasticity – a correlate of long-term potentiation-like visual cortex plasticity – is reported in SCZ_{spect} and BD (Cavus et al., 2012; Elvsashagen et al., 2012; Valstad et al., 2021; Zak et al., 2018). Reduced VEP amplitude (Bubl et al., 2015; Lubiński et al., 2023) and altered VEP plasticity (Normann et al., 2007b) is also described in major depression.

VEPs are event related potential (ERP) signals that reflect postsynaptic potentials generated by pyramidal cells in the visual cortex, and thus early visual sensory processing and the integrity of visual pathways (Shigihara et al., 2016). In humans, checkerboard reversal

* Corresponding author at: postal address: Norwegian centre for Mental Disorders Research, Oslo University Hospital, P.O. Box 4956 Nydalen, Norway.
E-mail address: n.b.slapo@medisin.uio.no (N.B. Slapø).

https://doi.org/10.1016/j.pscychresns.2023.111633
Received 13 January 2023; Received in revised form 12 March 2023; Accepted 17 March 2023
Available online 24 March 2023

stimulation triggers VEPs with three main components, the N75, the P100 and the N145 (Luck, 2014; Sarnthein et al., 2009), that can be extracted from scalp-recorded EEG. While the exact cortical sources of the VEP components remain to be fully clarified, previous studies suggest that the N75 component is generated mainly in the primary visual cortex (V1) area, while the P100 and N145 components are produced in both the V1 and the extrastriate visual cortices (Di Russo et al., 2002; Novitskiy et al., 2011). As illustrated in Fig. 1 checkerboard reversal stimulation triggers VEP responses that can be recorded with scalp-EEG. Altered VEP and visual processing deficits point toward involvement of the visual cortex in the pathogenesis of SCZ_{spect} and BD (Dudley et al., 2018; Ford et al., 2015; Klein et al., 2020).

Furthermore, while hallucinations are most frequently experienced in the auditory domain in SCZ_{spect}, it is estimated that 27% of patients experience visual hallucinations (Waters et al., 2014), often co-occurring with hallucinations in other sensory modalities (Lim et al., 2016). Previous studies indicate an association between altered structure in the visual system and altered visual processing (Reavis et al., 2017b), including visual hallucinations (Bernardin et al., 2020). However, how structure and function in the visual cortex in SCZ_{spect} and BD relate remains poorly understood (Reavis et al., 2020). Magnetic resonance imaging (MRI) studies show group-level alterations in brain cortical structure in SCZ_{spect} and BD (Abé et al., 2016; Elvsåshagen et al., 2013; Kim et al., 2020; Kuperberg et al., 2003; Madre et al., 2020; Rimol et al., 2012; van Erp et al., 2018; Zhu et al., 2022), including altered cortical surface area and thickness in V1. Previous studies using retinotopic mapping to define V1 areas reported thinner V1 in SCZ_{spect} compared with healthy controls (Reavis et al., 2017a). In a large-scale meta-analysis, the surface area and thickness of occipital regions were

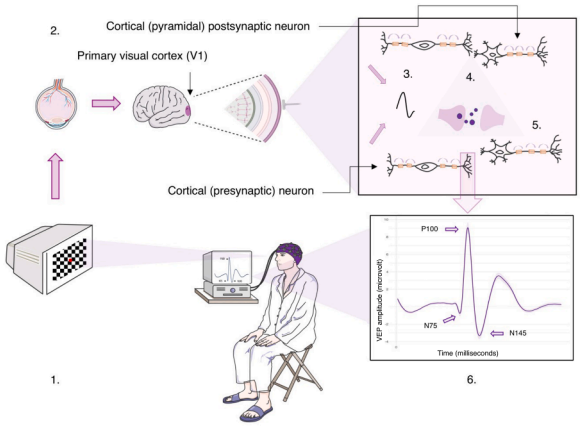

Fig. 1. The figure illustrates how visual stimuli in the form of checkerboard reversals stimulates the visual system all the way from the retina to the primary visual cortex (V1) and how the visual evoked potentials (VEPs) can be recorded with scalp-electroencephalography (EEG). Step 1: Scalp-EEG is recorded while the participant is focusing on a red dot in the middle of a computer screen (placed approximately 50 cm in front of them) while exposed to reversals of checkerboards. Step 2: The reversal of checkerboards (white squares change color to black and vice versa) stimulates the visual system to send electrical impulses from the retina, through the optic nerve and towards V1. Step 3: When the electrical impulses reach V1, presynaptic neurons (interneurons) generate action potentials (APs) that trigger the presynaptic cells to release neurotransmitters from the presynaptic terminals into the synaptic clefts. Step 4: Binding of the neurotransmitters to receptors on the postsynaptic neurons (pyramidal cells) generate temporary changes in the postsynaptic membrane potentials, also known as postsynaptic potentials (PSPs). Step 5: Summation of PSPs from a large number of synchronized pyramidal neurons can be recorded from scalp electrodes overlying the V1 area. Step 6: Grand average VEPs measured at the occipital (Oz) with anterior reference (AFz) during intervention phase of the first VEP paradigm that lasted for 10 min, yielding a total of 1200 reversals. Ms=milliseconds; μV=microvolts. Note: some parts of the symbols used in Fig. 1 are taken from Servier Medical Art.

both found to be reduced in SCZ_{spect} compared with healthy controls; however, no difference was observed after correcting for global differences (van Erp et al., 2018). One study reported associations between reduced V1 thickness and altered performance on a visual masking task in SCZ_{spect} (Reavis et al., 2017a) and several studies have investigated the relationship between brain structure and visual processing using various methods in SCZ_{spect}, BD, and in healthy controls (Genc et al., 2015; Lee et al., 2016; Reavis et al., 2020, 2017b; Schwarzkopf et al., 2012; Whittingstall et al., 2007).

However, studies utilizing the enhanced spatio-temporal resolution obtained when combining structural MRI (sMRI) and ERP techniques to explore how surface area and thickness in V1 relates to the VEP amplitude are lacking (Butler et al., 2005). One previous study from our research group found a positive correlation between the amplitude of the P100 component of the VEP and surface area in V1 (Elvsashagen et al., 2015) in a small sample of healthy individuals ($n = 39$), but no study has replicated this finding in a larger sample of healthy subjects.

Combining VEP and sMRI measures of V1 surface area and V1 thickness may provide new insights into neural substrates of functional alterations in the visual cortex in SCZ_{spect} and BD. Cortical surface area and thickness differ in their developmental trajectories (Amlien et al., 2016) and genetic underpinnings (Panizzon et al., 2009). Of note, there is evidence indicating that V1 surface area and thickness are differentially related to visual function: larger V1 surface area, but not thicker V1 cortex, was found to correlate with better performance on some visual tasks (Himmelberg et al., 2022; Song et al., 2015). To determine implications of visual cortex dysfunction in these patients, we also need to improve our understanding of the structure-function relationship in V1 in healthy individuals.

In the present study we included 307 healthy controls (HC) and patients with schizophrenia spectrum disorders (SCZ_{spect}, $n = 30$) or with bipolar disorders (BD, $n = 45$). All participants underwent sMRI and a VEP paradigm, as described previously (Elvsashagen et al., 2015; Normann et al., 2007a; Valstad et al., 2020, 2021). Here, VEPs are elicited at baseline, during an intervention block of prolonged visual stimulation, and post-intervention. The prolonged visual stimulation of the intervention block results in robust VEPs with a high signal-to-noise ratio; the P100 amplitude from these intervention block VEPs were used in the current work. The main aims of the present study were: 1) to compare P100 amplitude, V1 surface area and V1 thickness in HC, SCZ_{spect} and BD and 2) to examine the association between P100 amplitude and V1 structure, i.e., surface area and thickness in HC, SCZ_{spect} and BD. Based on previous reports, our primary hypothesis was that SCZ_{spect} and BD have smaller P100 amplitude, reduced V1 surface area and reduced V1 thickness compared to HC. Our secondary hypothesis, based on previous findings was that there was a positive association between P100 amplitude and V1 surface area, but not V1 thickness in HC (Elvsashagen et al., 2015).

2. Methods and materials

2.1. Participants

Patients with a DSM-IV diagnosis of SCZ_{spect} (including schizophrenia, schizophreniform, schizoaffective and psychotic disorder not otherwise specified (NOS)) or BD (including bipolar type 1, bipolar type 2 and bipolar NOS) were included from the ongoing Thematically Organized Psychosis (TOP) research study. HC were included from the TOP and the StrokeMRI studies conducted at the Norwegian Center of Mental Disorders (NORMENT) in Oslo, Norway. HC were either randomly drawn from the national population register, matched by age and region, or recruited through advertisement in local newspapers, social media, and word-of-mouth. Participants with a history of head trauma resulting in loss of consciousness, an IQ<70, or with somatic or neurological disorders believed to influence brain function, were excluded from the study. Additional exclusion criteria for HC were as

follows: 1) a history of mental disorders and/or severe mental disorders in first degree relatives, 2) a history of alcohol- and substance abuse or dependence 3) use of cannabis in the last three months prior to study inclusion. In addition, we excluded participants with clinically relevant incidental findings on their MRI scan, with poor quality of V1 area mask and with a time interval between the EEG recording and MRI scanning of more than 11 months. In the remaining sample, EEG and MRI data were collected between 2015 and 2019 with a median time interval between EEG and MRI examinations of 17 days (interquartile time difference of 40 days (time difference range of 0–321 days)). A large majority of the patients and controls of the present study were also part of a recently published work that reported evidence for impaired VEP plasticity in individuals with SCZspect and BD, when compared to HC (Valstad et al., 2021). Clinical examinations were performed during the same time period. An overview of the final study sample is provided in Table 1. The study was approved by the Regional Committees for Medical and Health Research Ethics of South – Eastern Norway, and was conducted in accordance with the Helsinki declaration. Participants provided written informed consent.

2.2. The visual evoked potential

The VEP paradigm was adopted from Normann et al. (Normann et al., 2007a) and procedures were performed as described previously (Elvsashagen et al., 2015; Valstad et al., 2020, 2021). In brief, over a period of 67 min, 11 VEP blocks including 2 baseline blocks, 1 intervention block of prolonged visual stimulation, and 8 postintervention blocks, were presented on a 24-inch 144 Hz AOC LCD screen with 1 ms gray-to-gray response time. All blocks, including the intervention block, consisted of a reversing checkerboard pattern with a spatial frequency of 1 cycle/degree over a ~28° visual angle. The VEPs were elicited by a checkerboard pattern with a fixed reversal frequency of 2 Hz in the intervention block, whereas the baseline and postintervention blocks had jittered stimulus onset asynchronies of 500–1500 ms (mean=1000 ms). All baseline and postintervention blocks lasted ~40 s (i.e., 40 checkerboard reversals), while the intervention block lasted 10 min (i.e., 1200 reversals). The prolonged visual stimulation of the intervention block resulted in VEPs with high signal-to-noise ratio and the intervention block VEPs were thus used for the analyses of the present study. Through all blocks, the participants fixed their gaze on a red dot in the center of the screen, and pressed a button on a gaming controller when the color of the dot changed from red to green. *Supplementary Figure 1* shows the timeline of the entire EEG session.

2.3. EEG acquisition, processing and quality control

We recorded EEG data at 2048 Hz from 64 Ag-AgCl scalp electrodes arranged according to the international 10–5 system using a BioSemi ActiveTwo amplifier. In addition, four external electrodes recorded lateral and vertical eye movements and two recorded the heart rhythm (electrocardiography). The Biosemi system uses a common mode sense with a driven right leg electrode in order to minimize common mode voltages. All offline EEG processing was conducted using the MATLAB-based EEGLAB toolbox (Delorme and Makeig, 2004). After down-sampling to 512 Hz, we removed noisy channels using the PREP Pipeline algorithms with default setting (Bigdely-Shamlo et al., 2015). We referenced remaining channels to the average of all good channels before we interpolated removed channels from surrounding channel potentials. Next, we re-referenced all channels to the new common average obtained after interpolation of bad channels. We then band-pass filtered EEG data between 0.1 and 40 Hz. A fixed 20 ms delay in the visual presentation relative to the event markers was detected using a BioSemi PIN diode placed in front of the screen while running the paradigm, and event markers were adjusted offline to account for this. Next, we extracted epochs at 200 ms pre- to 500 ms post-stimulus. EEG data was decomposed into independent components using the SOBI algorithm (Belouchrani et al., 1993) and muscle, eye blinks and eye movement artefacts were removed with SASICA (Chaumon et al., 2015) default settings. Then epochs with amplitude exceeding 100 μV were removed and the AFz electrode was used as the reference electrode for all channels. ERPs were extracted from the Oz channel. In the current study we focused on VEP elicited during the intervention phase of the VEP paradigm, lasting approximately 10 min and yielding a total of 1200 reversals of checkerboards with a fixed frequency of 2 reversals per second. We extracted N75, P100 and N145 amplitudes from the VEP. As a quality index for EEG, we computed the standard error (SE) (across trials) of VEP amplitudes (SE of N75, SE of P100 and SE of N145) for each participant, and standardized this index by dividing them by the mean VEP amplitudes (i.e., expressing the cross-trial variance as a percentage of the total amplitude) (Luck et al., 2021). While not common in EEG studies, a quality index essentially identical to the SE measure used in the current study was recently recommended by a leading EEG-researcher (Luck et al., 2021). More detail on this quality index is provided in *suppl. analysis 2.* Fig. 2.a. shows grand average VEP in HC (n = 307), SCZ_{spect} (n = 30) and BD while Fig. 2.b. shows preprocessed ERPs from each individual in each diagnostic group and grand average VEP in each group. Further, supplementary Figure 2 (a-b) illustrates preprocessed ERPs from 10 randomly drawn healthy controls (a) and from 5 randomly drawn patients (b).

Table 1
shows demographics of the final study sample including HC, healthy controls, SCZ_{spect}, patients with schizophrenia spectrum disorders; BD, patients with bipolar disorder. AGE, mean age with age range; sd, standard deviation; *, significant difference (p<0.003) between groups. Table 1 also shows mean sex distribution and age in HC, SCZ_{spect} and BD and differences in sex distribution and age between these groups. HC had significantly higher age compared to SCZ_{spect} and to BD.

	WOMEN, N (%)	AGE, MEAN (RANGE, SD)
HC [N = 307]	183 (59)	50 (18–85, 17)
SCZSPECT [N = 30]	17 (57)	33 (18–54, 10)
BD [N = 45]	31 (69)	33 (20–57, 11)
HC VS. SCZSPECT	p = 0.75	p = 3.23e-10*
HC VS. BD	p = 0.23	p = 2.35e-14*

2.4. MRI acquisition, processing and quality control

MRI scanning was performed with a General Electric Discovery MR750 3T scanner at the Regional Core Facility for Translational MRI Neuroimaging located at Oslo University Hospital. T1-weighted inversion recovery-prepared 3D gradient recalled echo volumes were acquired using the following parameters: 188 sagittal slices, field of view: 256 × 256 mm, voxel size: 1 × 1 × 1 mm, inversion time: 450 msec, echo time: 3.18 msec, repetition time: 8.16 msec, flip angle: 12° All MRI scans were processed using FreeSurfer version 6.0 (https://surfer.nmr.mgh.harvard.edu) (Fischl, 2012). In brief, processing steps included removal of non-brain tissue, automatic Talairach transformation and intensity correction. Intensity information was used to reconstruct the inner (i.e., the gray/white matter boundary) and outer (i.e., the gray matter/cerebrospinal fluid boundary) surface of the cerebral cortex through a series of processing steps as previously described (Dale et al., 1999; Fischl et al., 2004; Hinds et al., 2008). Similar to Elvsåshagen et al. (2015) (Elvsashagen et al., 2015), we adopted the methods from Hinds et al. (2008) (Hinds et al., 2008) to obtain measures of the left hemisphere (lh) V1 surface area, right hemisphere (rh) V1 surface area, lh V1 thickness and rh V1 thickness, in addition to estimated total intracranial volume (eTIV). This method located the V1 using a surface-based probabilistic atlas derived from high-resolution sMRI of the stria of Gennari. All surface reconstructions were inspected by trained research assistants. If errors in surface placements were detected, manual editing was performed according to standard FreeSurfer procedures (McCarthy et al., 2015). Surface editing was performed in 197 (51.6%) out of all images

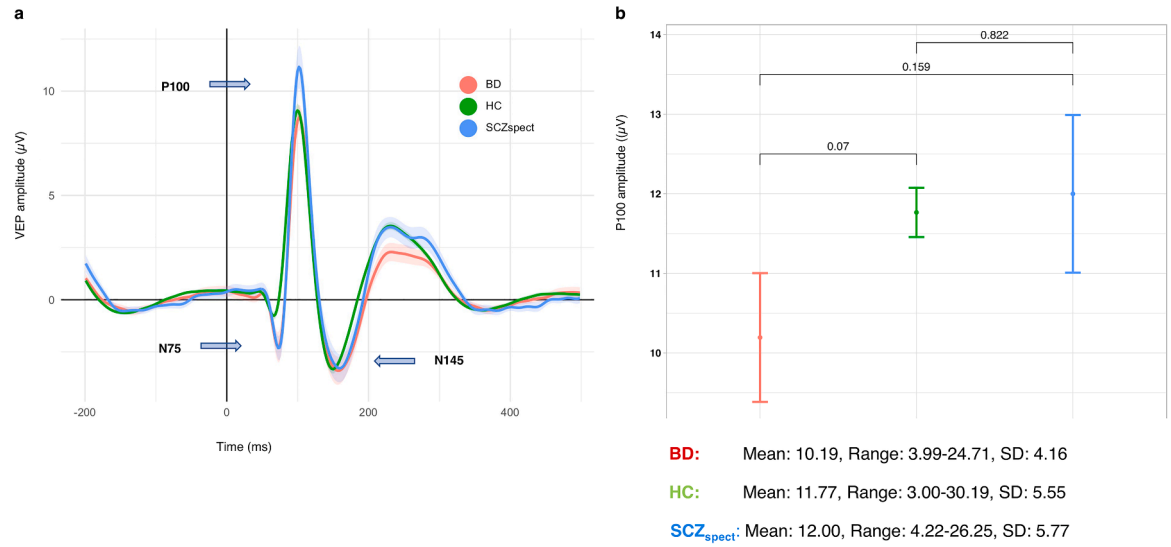

Fig. 2. (**a**) Grand average mean visual evoked potential (VEP) extracted from the intervention block in healthy controls (HC, $n = 307$), patients with schizophrenia spectrum disorders (SCZ_{spect}, $n = 30$) and patients with bipolar disorders (BD, $n = 45$). In this figure, the VEP are not corrected for age, sex or standard error (SE) for VEP amplitudes. The shadows represent standard error (SE) of the VEP. μV (microvolts); ms (milliseconds). (**b**) Mean P100 amplitude and differences in mean P100 amplitude between HC, SCZ_{spect} and BD. In this figure, P100 amplitudes are not corrected for age, sex or SE for P100 amplitude. Mean (mean P100 amplitude); Range (min-max P100 amplitude); SD (standard deviation). P100 amplitude (not corrected for age, sex or SE for P100 amplitude) was smallest in BD and largest in SCZ_{spect}, but did not differ between HC, SCZ_{spect} and BD.

($n = 382$) included in the current study. In addition to these quality assurance steps we included FreeSurfer Euler numbers (Euler) as covariates in our analyses to evaluate MRI image quality (Rosen et al., 2018). We calculated the "total corrected Euler number" from numbers of holes in the original (non-corrected) cortical surface, using the following formula: 2*(#holes −1) for both the left and right V1 surface area. Further, we calculated the total V1 surface area by summating lh V1 surface area and rh V1 surface area, while total V1 thickness was calculated as follows: total V1 thickness= ((lh V1 thickness*lh V1 surface area) + (rh V1 thickness*rh V1 surface area))/total V1 surface area.

2.5. Statistical analyses

Statistical analyses were conducted in R version 3.6. (https://www.r-project.org, R Core Team, 2014) and figures were created using the ggplot2 package in R (Wickham, 2016). Group differences in sex distribution and in age, were calculated using the chi-squared test for sex and the *t*-test for age (Table 1). Outliers were removed using the "Routliers" package implemented in R studio, which uses a default of 3.5 median absolute deviation as threshold to removed participants with deviating variables. Participants with P100 amplitude, V1 surface area, V1 thickness, eTIV, Euler numbers or standard error of the P100 amplitude that deviated with more than 3.5 from the median norm, were removed (*suppl. Note 1)*. The final study sample, after removing outliers, consisted of 382 participants, including 307 HC and 75 patients (30 with SCZ_{spect}: schizophrenia ($n = 18$), schizoaffective ($n = 3$), schizophreniform ($n = 1$) and psychosis NOS ($n = 8$); 45 with BD: BD type 1 ($n = 22$), BD type 2 ($n = 22$) and BD NOS ($n = 1$)). To compare P100 amplitude, V1 surface area and V1 thickness between HC and patients with SCZ_{spect} or BD, we performed analysis of covariance. Based on reports in the literature we decided to correct P100 amplitude for age (Celesia et al., 1987; Gupta and Deshpande, 2016) and sex (Avitabile et al., 2007; Celesia et al., 1987; Dotto et al., 2017; Gupta and Deshpande, 2016; Lancaster, 2016; Sharma et al., 2015); V1 surface area for age (Amunts et al., 2007; Barnes et al., 2010; Barta and Dazzan, 2003; Luders et al., 2006; Ritchie et al., 2018), sex (Amunts et al., 2007; Barnes et al., 2010; Barta and Dazzan, 2003; Luders et al., 2006; Ritchie et al., 2018) and eTIV (Barnes et al., 2010); and V1 thickness for age (Amunts et al., 2007; Barnes et al., 2010; Barta and Dazzan, 2003; Luders et al., 2006; Ritchie et al., 2018) and sex (Amunts et al., 2007; Barnes et al., 2010; Barta and Dazzan, 2003; Luders et al., 2006; Ritchie et al., 2018). Further, we controlled P100 amplitude for EEG quality measures, i.e., SE of P100 and V1 surface area and V1 thickness for MR quality control measures, i.e., Euler. First, P100 amplitude was set as outcome variable, diagnosis (HC/ SCZ_{spect} /BD) and sex as factors, and age and SE of P100 as covariates. Next, V1 surface area was set as outcome variable, diagnosis and sex as factors, and age, eTIV and Euler as covariates. Then, V1 thickness was set as outcome variable, diagnosis and sex as factors and age, and Euler as a covariate. Cohen's *d* for group comparisons was calculated from differences in predicted means (Thalheimer and Cook, 2009). To examine the associations between P100 amplitude and V1 structure, i.e., V1 surface area and V1 thickness we fitted linear regression models, for HC, SCZ_{spect} and BD separately. First, P100 amplitude was set as the dependent variable with age, sex, SE of P100 and V1 surface area as independent variables. Next, P100 amplitude was set as dependent variable with age, sex, SE of P100 and V1 thickness as independent variables. A Bonferroni corrected p-value<0.003 was considered significant for the main analyses.

In addition to our main analyses, we ran supplementary analyses to test for effects of covariates on P100 amplitude, V1 surface area/thickness, to test for effect of SE of P100 on V1 surface area /thickness, to examine V1 surface area/thickness for each hemisphere separately, to test differences in P100 amplitude, V1 surface area/thickness between HC and the combined sample of patients and to examine the associations between the amplitude of the other VEP components and V1 surface area/thickness. In addition, we examined mean P100 amplitude, V1 surface area and V1 thickness and differences in means between age-matched groups of HC, SCZ_{spect} and BD. We also examined the association between P100-V1 surface area/thickness in the age-matched HC sample. Last, we ran supplementary analysis to examine the association between P100 amplitude and surface across the whole cortex. Results are available in supplements.

3. Results

3.1. Demographics

3.2. P100 amplitude, V1 surface area and V1 thickness in HC, SCZ_{spect} and BD

Mean P100 amplitude, V1 surface area and V1 thickness in HC, SCZ_{spect} and BD and differences in means between HC and patients with SCZ_{spect} or BD are shown in Table 2. Associations between P100 amplitude and V1 surface area /thickness in HC, SCZ_{spect} and BD are shown in Figs. 3-5a-b. We found no significant difference in mean P100 amplitude, V1 surface area or V1 thickness between HC and patients with SCZ_{spect} or BD. However, in BD, P100 amplitude ($p = 0.04$, $d = 0.33$) and V1 surface area were nominally reduced ($p = 0.01$, $d = 0.44$) compared to HC, while V1 was nominally thicker ($p = 0.05$, $d = 0.25$) in BD compared to HC. In SCZ_{spect}, V1 was nominally thinner compared to HC ($p = 0.05$, $d = 0.25$). For HC only, P100 amplitude was positively associated with V1 surface area ($t = 3.57$, $p = 0.0004$).

In addition to our main results, our supplementary analyses revealed a significant negative effect of sex (male) on P100 amplitude in HC while SE for P100 amplitude had a significant negative effect on P100 amplitude in all groups. Further, in HC only, age had a significant negative effect on V1 surface area and V1 thickness, while eTIV had a significant positive effect on V1 surface area in all groups (Table S1). Our supplementary analyses revealed nominally thinner left V1 in SCZ_{spect} and nominally smaller left and right V1 surface area and P100 amplitude in BD compared to HC (Table S2). Further, we observed positive associations between P100 amplitude and left and the right V1 surface area in HC only (Table S3). Mean P100 amplitude, V1 surface area and V1 thickness did not differ significantly between HC and the combined sample of patients ($n = 75$) (Table S4). Further, mean N75 and N145 amplitudes did not significantly differ between HC and SCZ_{spect} or BD (Table S5) and were not associated with V1 surface area/thickness in any groups (Table S6). Further, V1 surface area was nominally reduced in BD, while V1 was significantly thinner in SCZ_{spect} compared to the age-matched sample of HC (Table S7). Further, P100 amplitude was nominally positively associated with V1 surface area, but not with V1 thickness in the age-matched HC group. Lastly, the vertex-wise whole brain analyses revealed nominally positive association between the P100 amplitude and V1 surface area (bilateral) (Figure S3).

4. Discussion

The current study yielded three main findings. First, P100 amplitude, V1 surface area and V1 thickness did not differ significantly between HC and patients with SCZ_{spect} or BD, in contrast to our hypothesis. However, BD had nominally smaller P100 amplitude, nominally reduced V1 surface area and nominally thicker V1 compared to HC. Further, in SCZ_{spect}, V1 was nominally thinner compared to HC. Second, there was a positive association between P100 amplitude and V1 surface area, but not V1 thickness, in HC, which was in line with our secondary hypothesis. Third, we did not find any association between P100 amplitude and V1 surface area/thickness in SCZ_{spect} or BD. However, given the limited number of patients included in the current study there is need for careful interpretation of these results.

The exact mechanism behind the positive P100-V1 surface area association in healthy individuals remains elusive. However, the pool of synapses and the width and/or the number of cortical columns in V1 potentially increases with enlarged surface area, enhancing the summation of postsynaptic potentials (PSP) generated by V1 pyramidal neurons. Since the P100 amplitude primarily reflects PSP generated by V1 pyramidal cells, a greater summation of PSP with a larger surface area may explain the current findings of a positive P100-V1 surface area association in controls (Schwarzkopf et al., 2012). Further, the level of axonal myelination in V1 may correlate with V1 surface area in controls. Further, enhanced axonal myelination with larger V1 surface area may enable V1 neurons to fire more synchronously (Dutta et al., 2018; Ishibashi et al., 2006; Pajevic et al., 2014; Schwarzkopf et al., 2012; Zalc and Fields, 2000). As scalp EEG reflect only synchronized neuronal activity, a larger surface area and enhanced myelination in V1 may result in a larger P100 amplitude. Further, the level of myelination influences the conduction velocity of action potentials (AP) through presynaptic axons. If APs from a large group of presynaptic cells arrive at the presynaptic terminal simultaneously, neurotransmitters are released from the presynaptic cell into the synaptic cleft, bind to the receptors on the postsynaptic pyramidal neurons and generate PSPs. The summation of PSPs from large groups of synchronized neurons can be recorded with scalp-EEG. Thus, an increased P100 amplitude may reflect enhanced

Table 2
Shows mean P100 amplitude and mean surface area and thickness in the V1, primary visual cortex in HC, healthy controls, in SCZ_{spect}, patients with schizophrenia spectrum disorders and in BD, patients with bipolar disorders. Estimated marginal means were calculated using ANCOVA, where P100 amplitude, V1 surface area or V1 thickness were set as dependent variables with age, sex and diagnosis as independent variables. For P100 amplitude, standard error for P100 amplitude was included as an additional covariate, while for V1 surface area, estimated total intracranial volume and Euler number were included as additional covariates. For V1 thickness Euler number was included as an additional covariate. Estimated marginal means are provided with SE (standard error of the mean) and 95% CI, confidence interval. In addition, table 2 shows differences in mean P100 amplitude, V1 surface area and V1 thickness between HC and SCZ_{spect} and between HC and BD. Est, estimate; t, t-value; p, p-value; df, degree of freedom; *, significant ($p<0.003$) difference between groups. We found no significant difference in mean P100 amplitude, V1 surface area or V1 thickness between HC and patients with SCZ_{spect} or BD.

	P100 AMPLITUDE (microvolts) MEAN (SE) [95% CI]	V1 SURFACE AREA (mm^2) MEAN (SE) [95% CI]	V1 THICKNESS (mm) MEAN (SE) [95% CI]
HC [$N = 307$]	11.53 (0.22)	4802.06 (31.96)	1.84 (0.01)
	[11.10–11.95]	[4739.21–4864.91]	[1.83–1.86]
SCZSPECT [$N = 30$]	12.35 (0.69)	4854.97 (101.55)	1.80 (0.02)
	[10.99–13.71]	[655.30–5054.65]	[1.75–1.84]
BD [$N = 45$]	10.24 (0.58)	4551.75 (85.12)	1.88 (0.02)
	[9.10–11.38]	[4384.39–4719.12]	[1.85–1.92]
HC VS. SCZSPECT	est=−0.82	est=−52.91	est=0.05
	se=0.73	se=107.35	se=0.02
	$t = 1.12$	t=−0.49	$t = 2.01$
	$p = 0.26$	$p = 0.62$	$p = 0.05$
	df=376	df=375	df=376
	Cohen's $d = 0.21$	Cohen's $d = 0.09$	Cohen's $d = 0.36$
HC VS. BD	est=−1.29	est=−250.31	est=0.04
	se=0.62	se=91.45	se=0.02
	t=−2.07	t=−2.74	$t = 1.99$
	$p = 0.04$	$p = 0.01$	$p = 0.05$
	df=376	df=375	df=376
	Cohen's $d = 0.33$	Cohen's $d = 0.44$	Cohen's $d = 0.25$

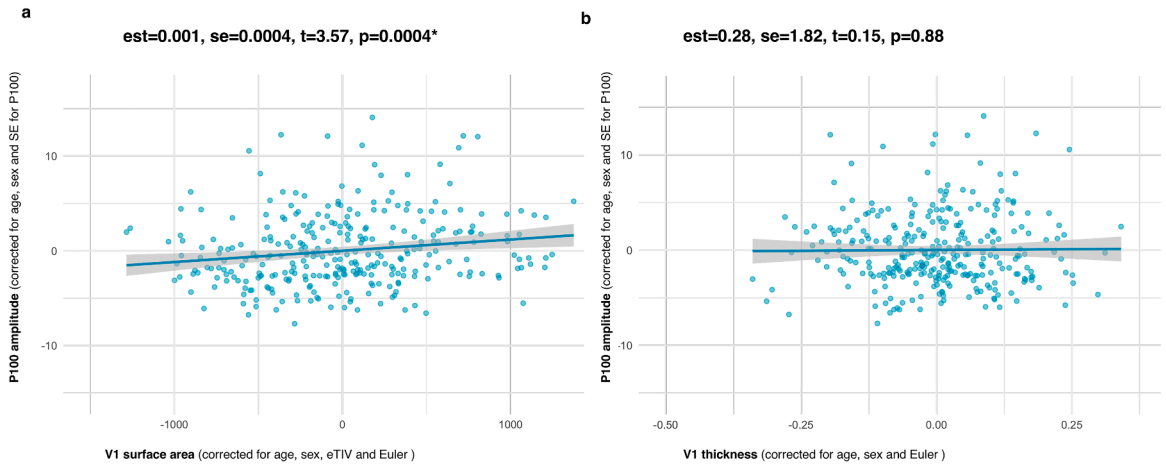

Fig. 3. Shows association between **(a)** P100 amplitude and V1, primary visual cortex, surface area and **(b)** between P100 amplitude and V1 thickness in healthy controls [$n = 307$]. Est, estimate; se, standard error; t, t-value; p, p-value; *, significant ($p<0.003$) associations. In healthy controls, P100 amplitude was positively associated with V1 surface area.

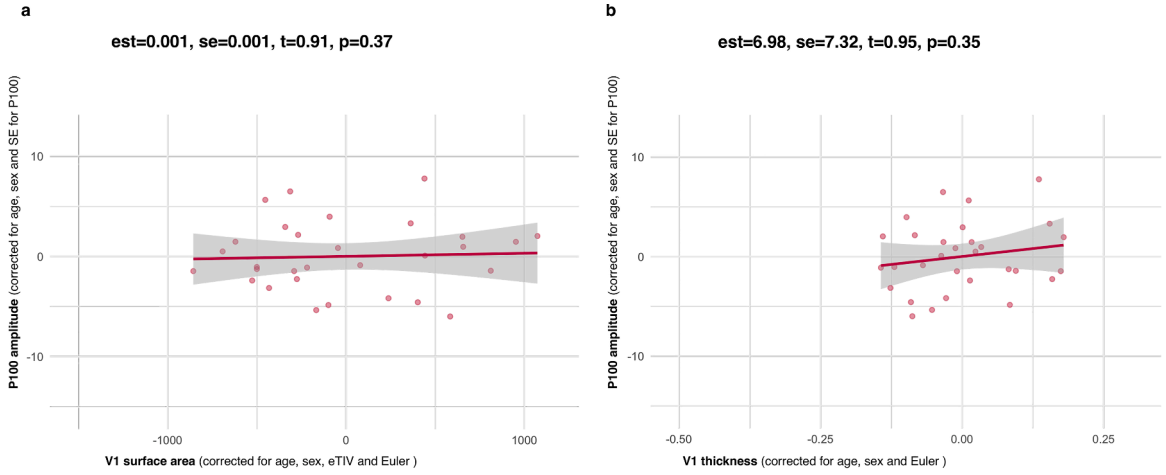

Fig. 4. Shows association between **(a)** P100 amplitude and V1, primary visual cortex, surface area and **(b)** between P100 amplitude and V1 thickness in patients with schizophrenia spectrum disorders (SCZ_{spect}, $n = 30$). Est, estimate; se, standard error; t, t-value; p, p-value; *, significant ($p<0.003$) associations. In patients with schizophrenia spectrum disorder, we found no significant association between P100 amplitude and V1 surface area or between P100 amplitude and V1 thickness.

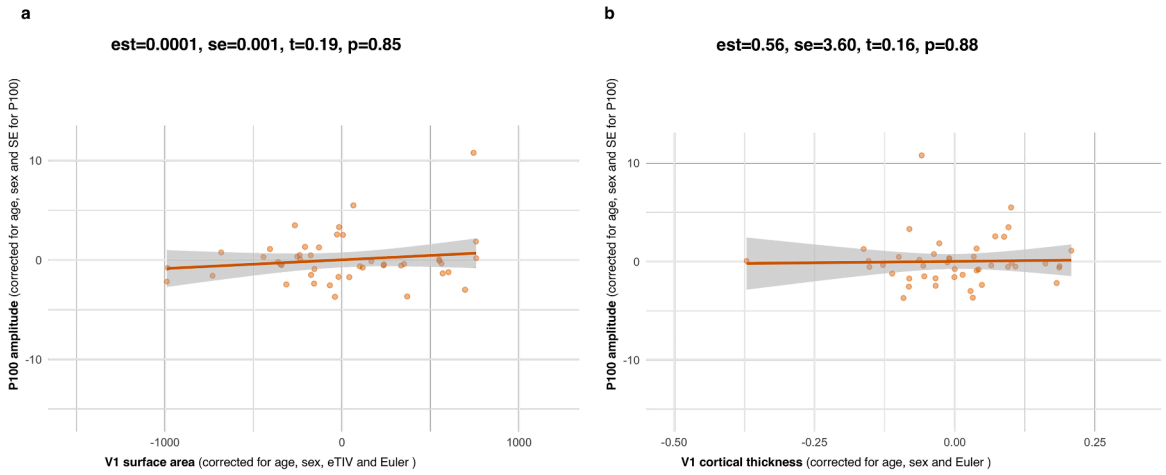

Fig. 5. Shows association between **(a)** P100 amplitude and V1, primary visual cortex, surface area and **(b)** between P100 amplitude and V1 thickness in patients with bipolar disorder [$n = 45$]. Est, estimate; se, standard error; t, t-value; p, p-value; *, significant ($p<0.003$) associations. In patients with bipolar disorder, we found no significant association between P100 amplitude and V1 surface area or between P100 amplitude and V1 thickness.

summation of PSPs in V1. Since the V1 is highly myelinated, the level of myelination in V1 may mirror function in the same area as reflected by P100 amplitude, either by enhancing summation of PSPs or indirectly by increasing the diameter of pyramidal axons, or both (Dinse et al., 2015; Dutta et al., 2018; Pajevic et al., 2014; Zalc and Fields, 2000). Exactly how myelination in V1 mirrors P100 amplitude remains elusive. Further, the level of neurotransmitters released by presynaptic neurons, i.e., glutamate or gamma aminobutyric acid (GABA) may impact the generation of PSPs (Martin R. Gluck et al., 2002; Romanos et al., 2019). Thus, in theory, a larger number of synapses in V1, with increased V1 surface area, may enhance the release of excitatory neurotransmitters (glutamate) and augmented summation of PSPs and larger P100 amplitude.

Current and previous evidence for an association between the P100 amplitude and the surface area, but not the thickness of V1 in healthy subjects indicate that surface area and thickness may influence cortical function in different ways. Cortical surface area and thickness are both heritable traits, but differ phenotypically and genetically and result from different ontogenetic stages during cortical development (Grasby et al., 2020; Norbom et al., 2021; Panizzon et al., 2009; Pontious et al., 2008; Strike et al., 2019; Wierenga et al., 2014). While cortical surface area appears more determined by genetics and early neurodevelopmental factors, cortical thickness is considered to be influenced by environmental and neurodegenerative factors (Panizzon et al., 2009; Strike et al., 2019; Wierenga et al., 2014; Winkler et al., 2010). Further, cortical surface area is determined by the total number of cortical columns while thickness is associated with the number of cells within each cortical column (Rakic, 1995). Thus, the current findings of a positive association between P100 amplitude and V1 surface area in healthy subjects, may be due to the organization of the cortex in columns and lamina, where the number and/or width of vertical columns correlate positively with surface area, but not thickness in V1 (Rakic, 1995).

One previous study that found a relationship between cortical surface area, but not thickness, and the gamma-band frequency EEG signal in healthy subjects, argued that the distance across the cortical sheet, rather than the gray matter volume determined this structure-function association (Schwarzkopf et al., 2012). Although speculative, considering that a larger cortical surface area in V1 reflect an increased number of vertically organized pyramidal cells while a thicker V1 mirrors increased length of pyramidal axons, increased V1 surface area, but not increased V1 thickness, would result in enhanced PSPs and larger P100 amplitude. Intriguingly, one of few previous ERP-MRI studies revealed a negative association between the amplitude of the N100 component of the auditory evoked potential, an ERP component reflecting function in the auditory cortex, and the thickness, but not surface area, in the auditory cortex (Liem et al., 2012) These findings support previous reports of a positive association between thinner cortex and function in the auditory cortex (Hyde et al., 2007; Liem et al., 2012). Albeit findings of a positive correlation between N100 amplitude and thickness in the auditory cortex is not directly comparable to the current study findings, they may suggest that increased surface area and thinner cortex mirror increased neural activity in some cortical brain areas (Hogstrom et al., 2013).

Based on reports of reduced P100 amplitude (Butler et al., 2007; Foxe et al., 2001; Yeap et al., 2008, 2006) in SCZ_{spect}, altered VEP plasticity in SCZ_{spect} and BD (Elvsashagen et al., 2012; Valstad et al., 2021; Zak et al., 2018) and widespread cortical thinning and reduced surface area, although not always reported specifically in V1, in SCZ_{spect} and BD (van Erp et al., 2018), we expected to find smaller P100 amplitude, reduced V1 surface area and thinner V1 in our patients compared to HC. However, in contrast to our primary hypothesis, we did not find any significant difference in mean P100 amplitude, V1 surface area or V1 thickness between HC and SCZ_{spect} or BD. Further, we found no significant association between P100 amplitude and V1 surface area/thickness in these patients. Additional studies with larger sample sizes are needed to eventually determine the relationship between P100-V1 surface area/thickness in SCZ_{spect} and BD. Other factors that may contribute to V1 dysfunction in SCZ_{spect} and BD, manifested as visual hallucinations, altered visual processing and altered VEP, include reduced V1 vol (Dorph-Petersen et al., 2007), reduced number of V1 cells (Dorph-Petersen et al., 2007) and altered morphology of pyramidal V1 cells (Mavroudis et al., 2021). However, whether and how these structural and morphological alterations in V1 relate to V1 function, as reflected by VEP, remains unknown. Synaptic dysfunction (Faludi and Mirnics, 2011), aberrant synchronization (Spencer et al., 2003; Uhlhaas and Singer, 2006) abnormal regulation of neurotransmitters (Ashok et al., 2017; Martin R. Gluck et al., 2002; Yoon et al., 2010) and/or abnormal myelination in V1 (Du et al., 2013; Jorgensen et al., 2016; Kelly et al., 2018; Takahashi et al., 2011) may also explain altered function in V1 in these patients. In particular, while previous studies show evidence for altered myelination in the visual cortex in SCZ_{spect} and BD (Du et al., 2013; Jorgensen et al., 2016; Kelly et al., 2018; Takahashi et al., 2011), whether and how myelination in V1 relates to VEP, remains unknown. Further, diminished dendritic arborization of V1 neurons and altered synaptic pruning in SCZ_{spect} may result in reduced summation of PSPs and hence smaller VEP (and P100) amplitude. Since the process of synaptic pruning is preceded by the development of the cortex (including V1 surface area and thickness) abnormal synaptic pruning might explain altered VEP with normal V1 surface area and V1 thickness in SCZ_{spect} and BD (Konopaske et al., 2014; Paolicelli et al., 2011; Sellgren et al., 2019). Studies examining the exact mechanisms to which all factors mentioned above might influence VEP (and P100) characteristics are missing. Knowledge on how these (structural) factors influence function in V1 may provide new insight into the neural substrates of altered brain function in severe mental disorders.

Some limitations have to be considered when interpreting the current findings. First, the small sample of patients may increase the risk of type 1 and type 2 errors. Further, we were not able to control for potential effects of skull thickness, cerebrospinal fluid and meninges on the conductance of electromagnetic fields from their neural sources to scalp electrodes. This should preferably be accounted for when analyzing ERP data. In addition, we did not control for medication use in our patient groups.

In conclusion, we confirmed previous findings of a positive association between P100 amplitude and V1 surface area, but not V1 thickness, in healthy individuals. However, for patients with SCZ_{spect} and BD, we did not find any significant associations between P100 amplitude and V1 surface area or between P100 amplitude and V1 thickness. Larger patient samples are needed to gain insight into neural substrates of altered V1 function in patients with severe mental disorders.

Author contributions

Nora Berz Slapø: conceptualization, methodology, formal analysis, investigation, visualization and writing original draft.

Kjetil Nordbø Jørgensen: conceptualization, MRI data acquisition and processing and supervision

Torbjørn Elvsåshagen: conceptualization, EEG data acquisition and supervision

Torgeir Moberget: conceptualization and supervision

Stener Nerland: MRI data acquisition and processing

Daniel Roelfs: EEG data acquisition

Mathias Valstad: EEG data acquisition, processing and visualization of EEG data

Clara M. F. Timpe: EEG data acquisition

Geneviève Richard: MRI and EEG data acquisition

Dani Beck: MRI data acquisition

Linn Sofie Sæther: EEG data acquisition

Maren C. Frogner Werner: Clinical inclusion

Trine Vik Lagerberg: Project administration

Ingrid Melle: Project administration

Ingrid Agartz: Project administration

Lars T. Westlye: Project administration

Ole A. Andreassen: conceptualization and project administration

Erik G. Jönsson: project administration, conceptualization, methodology and supervision

All co-authors contributed with review and editing of manuscript.

Declaration of Competing Interest

T.E. is a consultant to BrainWaveBank and Synovion and received speaker's honoraria from Lundbeck and Janssen Cilag. O.A.A. is a consultant to HealthLytix and received speaker's honoraria from Lundbeck. I.A. has received speaker's honoraria from Lundbeck. The other authors have no conflict of interest to report.

Acknowledgements

The study was funded by the Research Council of Norway (223273, 274359, 249795, 248238), the South – Eastern Norway Regional Health Authority (2014097, 2015044, 2015073, 2017097, 2018037, 2018076), the Norwegian Extra Foundation for Health and Rehabilitation (2015/FO5146), the European Research Council under the European Union's Horizon 2020 research and Innovation program (ERC StG 802998), the Ebbe Frøland foundation and a research grant from Mrs. Throne-Holst. MRI and EEG data used in the following study is currently not openly available due to ethical and privacy issues of clinical data.

Supplementary materials

Supplementary material associated with this article can be found, in the online version, at doi:10.1016/j.pscychresns.2023.111633.

Reference

Abé, C., Ekman, C.J., Sellgren, C., Petrovic, P., Ingvar, M., Landén, M., 2016. Cortical thickness, volume and surface area in patients with bipolar disorder types I and II. J. Psychiatry Neurosci. 41, 240–250.

Amlien, I.K., Fjell, A.M., Tamnes, C.K., Grydeland, H., Krogsrud, S.K., Chaplin, T.A., Rosa, M.G.P., Walhovd, K.B., 2016. Organizing principles of human cortical development–thickness and area from 4 to 30 years: insights from comparative primate neuroanatomy. Cereb. Cortex 26, 257–267.

Amunts, K., Armstrong, E., Malikovic, A., Homke, L., Mohlberg, H., Schleicher, A., Zilles, K., 2007. Gender-specific left-right asymmetries in human visual cortex. J. Neurosci. 27, 1356–1364.

Ashok, A.H., Marques, T.R., Jauhar, S., Nour, M.M., Goodwin, G.M., Young, A.H., Howes, O.D., 2017. The dopamine hypothesis of bipolar affective disorder: the state of the art and implications for treatment. Mol. Psychiatry 22, 666–679.

Avitabile, T., Longo, A., Caruso, S., Gagliano, C., Amato, R., Scollo, D., Lopes, R., Pulvirenti, L., Toto, L., Torrisi, B., Agnello, C., 2007. Changes in visual evoked potentials during the menstrual cycle in young women. Curr. Eye Res. 32, 999–1003.

Barnes, J., Ridgway, G.R., Bartlett, J., Henley, S.M.D., Lehmann, M., Hobbs, N., Clarkson, M.J., MacManus, D.G., Ourselin, S., Fox, N.C., 2010. Head size, age and gender adjustment in MRI studies: a necessary nuisance? Neuroimage 53, 1244–1255.

Barta, P., Dazzan, P., 2003. Hemispheric surface area: sex, laterality and age effects. Cereb. Cortex 13, 364–370.

Belouchrani, A., abed-meraim, K., Cardoso, J.F., Moulines, E., 1993. Second order blind separation of temporally correlated sources. In: Proceeding of the International Conference on Digital Signal Processing.

Bernardin, F., Schwitzer, T., Angioi-Duprez, K., Giersch, A., Jansen, C., Schwan, R., Laprevote, V., 2020. Retinal ganglion cells dysfunctions in schizophrenia patients with or without visual hallucinations. Schizophr. Res. 219, 47–55.

Bigdely-Shamlo, N., Mullen, T., Kothe, C., Su, K.M., Robbins, K.A., 2015. The PREP pipeline: standardized preprocessing for large-scale EEG analysis. Front. Neuroinform. 9, 16.

Birur, B., Kraguljac, N.V., Shelton, R.C., Lahti, A.C., 2017. Brain structure, function, and neurochemistry in schizophrenia and bipolar disorder-a systematic review of the magnetic resonance neuroimaging literature. NPJ Schizophr. 3, 15.

Bubl, E., Kern, E., Ebert, D., Riedel, A., Tebartz van Elst, L., Bach, M., 2015. Retinal dysfunction of contrast processing in major depression also apparent in cortical activity. Eur. Arch. Psychiatry Clin. Neurosci. 265, 343–350.

Butler, P.D., Martinez, A., Foxe, J.J., Kim, D., Zemon, V., Silipo, G., Mahoney, J., Shpaner, M., Jalbrzikowski, M., Javitt, D.C., 2007. Subcortical visual dysfunction in schizophrenia drives secondary cortical impairments. Brain 130, 417–430.

Butler, P.D., Zemon, V., Schechter, I., Saperstein, A.M., Hoptman, M.J., Lim, K.O., Revheim, N., Silipo, G., Javitt, D.C., 2005. Early-stage visual processing and cortical amplification deficits in schizophrenia. Arch. Gen. Psychiatry 62, 495–504.

Cavus, I., Reinhart, R.M., Roach, B.J., Gueorguieva, R., Teyler, T.J., Clapp, W.C., Ford, J. M., Krystal, J.H., Mathalon, D.H., 2012. Impaired visual cortical plasticity in schizophrenia. Biol. Psychiatry 71, 512–520.

Celesia, G.G., Kaufman, D., Cone, S., 1987. Effects of age and sex on pattern electroretinograms and visual evoked potentials. Electroencephalogr. Clin. Neurophysiol. 68, 161–171.

Chaumon, M., Bishop, D.V.M., Busch, N.A., 2015. A practical guide to the selection of independent components of the electroencephalogram for artifact correction. J. Neurosci. Methods 250, 47–63.

Dale, A.M., Fischl, B., Sereno, M.I., 1999. Cortical surface-based analysis: I. Segmentation and surface reconstruction. Neuroimage 9, 179–194.

Delorme, A., Makeig, S., 2004. EEGLAB: an open source toolbox for analysis of single-trial EEG dynamics including independent component analysis. J. Neurosci. Methods 134, 9–21.

Di Russo, F., Martínez, A., Sereno, M.I., Pitzalis, S., Hillyard, S.A., 2002. Cortical sources of the early components of the visual evoked potential. Hum. Brain Mapp. 15, 95–111.

Dinse, J., Härtwich, N., Waehnert, M.D., Tardif, C.L., Schäfer, A., Geyer, S., Preim, B., Turner, R., Bazin, P.L., 2015. A cytoarchitecture-driven myelin model reveals area-specific signatures in human primary and secondary areas using ultra-high resolution in-vivo brain MRI. Neuroimage 114, 71–87.

Dondé, C., Avissar, M., Weber, M.M., Javitt, D.C., 2019. A century of sensory processing dysfunction in schizophrenia. Eur. Psychiatry 59, 77–79.

Doniger, G.M., Foxe, J.J., Murray, M.M., Higgins, B.A., Javitt, D.C., 2002. Impaired visual object recognition and dorsal/ventral stream interaction in schizophrenia. Arch. Gen. Psychiatry 59, 1011–1020.

Dorph-Petersen, K.A., Pierri, J.N., Wu, Q., Sampson, A.R., Lewis, D.A., 2007. Primary visual cortex volume and total neuron number are reduced in schizophrenia. J. Comp. Neurol. 501, 290–301.

Dotto, P.F., Berezovsky, A., Sacai, P.Y., Rocha, D.M., Salomao, S.R., 2017. Gender-based normative values for pattern-reversal and flash visually evoked potentials under binocular and monocular stimulation in healthy adults. Doc. Ophthalmol. 135, 53–67.

Du, F., Cooper, A.J., Thida, T., Shinn, A.K., Cohen, B.M., Öngür, D., 2013. Myelin and axon abnormalities in schizophrenia measured with magnetic resonance imaging techniques. Biol. Psychiatry 74, 451–457.

Dudley, R., Aynsworth, C., Cheetham, R., McCarthy-Jones, S., Collerton, D., 2018. Prevalence and characteristics of multi-modal hallucinations in people with psychosis who experience visual hallucinations. Psychiatry Res. 269, 25–30.

Dutta, D.J., Woo, D.H., Lee, P.R., Pajevic, S., Bukalo, O., Huffman, W.C., Wake, H., Basser, P.J., SheikhBahaei, S., Lazarevic, V., Smith, J.C., Fields, R.D., 2018. Regulation of myelin structure and conduction velocity by perinodal astrocytes. Proc. Natl. Acad. Sci. 115, 11832–11837.

Elvsashagen, T., Moberget, T., Boen, E., Boye, B., Englin, N.O., Pedersen, P.O., Andreassen, O.A., Dietrichs, E., Malt, U.F., Andersson, S., 2012. Evidence for impaired neocortical synaptic plasticity in bipolar II disorder. Biol. Psychiatry 71, 68–74.

Elvsashagen, T., Moberget, T., Boen, E., Hol, P.K., Malt, U.F., Andersson, S., Westlye, L. T., 2015. The surface area of early visual cortex predicts the amplitude of the visual evoked potential. Brain Struct. Funct. 220, 1229–1236.

Elvsåshagen, T., Westlye, L.T., Bøen, E., Hol, P.K., Andreassen, O.A., Boye, B., Malt, U.F., 2013. Bipolar II disorder is associated with thinning of prefrontal and temporal cortices involved in affect regulation. Bipolar. Disord. 15, 855–864.

Faludi, G., Mirnics, K., 2011. Synaptic changes in the brain of subjects with schizophrenia. Int. J. Dev. Neurosci. 29, 305–309.

Fischl, B., 2012. FreeSurfer. Neuroimage 62, 774–781.

Fischl, B., van der Kouwe, A., Destrieux, C., Halgren, E., Segonne, F., Salat, D.H., Busa, E., Seidman, L.J., Goldstein, J., Kennedy, D., Caviness, V., Makris, N., Rosen, B., Dale, A. M., 2004. Automatically parcellating the human cerebral cortex. Cereb. Cortex 14, 11–22.

Ford, J.M., Palzes, V.A., Roach, B.J., Potkin, S.G., van Erp, T.G., Turner, J.A., Mueller, B. A., Calhoun, V.D., Voyvodic, J., Belger, A., Bustillo, J., Vaidya, J.G., Preda, A., McEwen, S.C., , Functional Imaging Biomedical Informatics Research, N., Mathalon, D.H., 2015. Visual hallucinations are associated with hyperconnectivity between the amygdala and visual cortex in people with a diagnosis of schizophrenia. Schizophr. Bull. 41, 223–232.

Foxe, J.J., Doniger, G.M., Javitt, D.C., 2001. Early visual processing deficits in schizophrenia: impaired P1 generation revealed by high-density electrical mapping. Neuroreport 12, 3815–3820.

Foxe, J.J., Murray, M.M., Javitt, D.C., 2005. Filling-in in schizophrenia: a high-density electrical mapping and source-analysis investigation of illusory contour processing. Cereb. Cortex 15, 1914–1927.

Genc, E., Bergmann, J., Singer, W., Kohler, A., 2015. Surface area of early visual cortex predicts individual speed of traveling waves during binocular rivalry. Cereb. Cortex 25, 1499–1508.

Grande, I., Berk, M., Birmaher, B., Vieta, E., 2016. Bipolar disorder. Lancet 387, 1561–1572.

Grasby, K.L., Jahanshad, N., Painter, J.N., Colodro-Conde, L., Bralten, J., Hibar, D.P., Lind, P.A., Pizzagalli, F., Ching, C.R.K., McMahon, M.A.B., Shatokhina, N., Zsembik, L.C.P., Thomopoulos, S.I., Zhu, A.H., Strike, L.T., Agartz, I., Alhusaini, S., Almeida, M.A.A., Alnæs, D., Amlien, I.K., Andersson, M., Ard, T., Armstrong, N.J., Ashley-Koch, A., Atkins, J.R., Bernard, M., Brouwer, R.M., Buimer, E.E.L., Bülow, R., Bürger, C., Cannon, D.M., Chakravarty, M., Chen, Q., Cheung, J.W., Couvy-Duchesne, B., Dale, A.M., Dalvie, S., de Araujo, T.K., de Zubicaray, G.I., de Zwarte, S. M.C., den Braber, A., Doan, N.T., Dohm, K., Ehrlich, S., Engelbrecht, H.R., Erk, S., Fan, C.C., Fedko, I.O., Foley, S.F., Ford, J.M., Fukunaga, M., Garrett, M.E., Ge, T.,

Giddaluru, S., Goldman, A.L., Green, M.J., Groenewold, N.A., Grotegerd, D., Gurholt, T.P., Gutman, B.A., Hansell, N.K., Harris, M.A., Harrison, M.B., Haswell, C. C., Hauser, M., Herms, S., Heslenfeld, D.J., Ho, N.F., Hoehn, D., Hoffmann, P., Holleran, L., Hoogman, M., Hottenga, J.J., Ikeda, M., Janowitz, D., Jansen, I.E., Jia, T., Jockwitz, C., Kanai, R., Karama, S., Kasperaviciute, D., Kaufmann, T., Kelly, S., Kikuchi, M., Klein, M., Knapp, M., Knodt, A.R., Krämer, B., Lam, M., Lancaster, T.M., Lee, P.H., Lett, T.A., Lewis, L.B., Lopes-Cendes, I., Luciano, M., Macciardi, F., Marquand, A.F., Mathias, S.R., Melzer, T.R., Milaneschi, Y., Mirza-Schreiber, N., Moreira, J.C.V., Mühleisen, T.W., Müller-Myhsok, B., Najt, P., Nakahara, S., Nho, K., Olde Loohuis, L.M., Orfanos, D.P., Pearson, J.F., Pitcher, T.L., Pütz, B., Quidé, Y., Ragothaman, A., Rashid, F.M., Reay, W.R., Redlich, R., Reinbold, C.S., Repple, J., Richard, G., Riedel, B.C., Risacher, S.L., Rocha, C.S., Mota, N.R., Salminen, L., Saremi, A., Saykin, A.J., Schlag, F., Schmaal, L., Schofield, P.R., Secolin, R., Shapland, C.Y., Shen, L., Shin, J., Shumskaya, E., Sønderby, I.E., Sprooten, E., Tansey, K.E., Teumer, A., Thalamuthu, A., Tordesillas-Gutiérrez, D., Turner, J.A., Uhlmann, A., Vallerga, C.L., van der Meer, D., van Donkelaar, M.M.J., van Eijk, L., van Erp, T.G.M., van Haren, N.E.M., van Rooij, D., van Tol, M.J., Veldink, J.H., Verhoef, E., Walton, E., Wang, M., Wang, Y., Wardlaw, J.M., Wen, W., Westlye, L.T., Whelan, C.D., Witt, S.H., Wittfeld, K., Wolf, C., Wolfers, T., Wu, J.Q., Yasuda, C.L., Zaremba, D., Zhang, Z., Zwiers, M.P., Artiges, E., Assareh, A.A., Ayesa-Arriola, R., Belger, A., Brandt, C.L., Brown, G.G., Cichon, S., Curran, J.E., Davies, G.E., Degenhardt, F., Dennis, M.F., Dietsche, B., Djurovic, S., Doherty, C.P., Espiritu, R., Garijo, D., Gil, Y., Gowland, P.A., Green, R. C., Häusler, A.N., Heindel, W., Ho, B.C., Hoffmann, W.U., Holsboer, F., Homuth, G., Hosten, N., Jack Jr., C.R., Jang, M., Jansen, A., Kimbrel, N.A., Kolskår, K., Koops, S., Krug, A., Lim, K.O., Luykx, J.J., Mathalon, D.H., Mather, K.A., Mattay, V.S., Matthews, S., Mayoral Van Son, J., McEwen, S.C., Melle, I., Morris, D.W., Mueller, B. A., Nauck, M., Nordvik, J.E., Nöthen, M.M., O'Leary, D.S., Opel, N., Martinot, M.P., Pike, G.B., Preda, A., Quinlan, E.B., Rasser, P.E., Ratnakar, V., Reppermund, S., Steen, V.M., Tooney, P.A., Torres, F.R., Veltman, D.J., Voyvodic, J.T., Whelan, R., White, T., Yamamori, H., Adams, H.H.H., Bis, J.C., Debette, S., Decarli, C., Fornage, M., Gudnason, V., Hofer, E., Ikram, M.A., Launer, L., Longstreth, W.T., Lopez, O.L., Mazoyer, B., Mosley, T.H., Roshchupkin, G.V., Satizabal, C.L., Schmidt, R., Seshadri, S., Yang, Q., Alvim, M.K.M., Ames, D., Anderson, T.J., Andreassen, O.A., Arias-Vasquez, A., Bastin, M.E., Baune, B.T., Beckham, J.C., Blangero, J., Boomsma, D.I., Brodaty, H., Brunner, H.G., Buckner, R.L., Buitelaar, J. K., Bustillo, J.R., Cahn, W., Cairns, M.J., Calhoun, V., Carr, V.J., Caseras, X., Caspers, S., Cavalleri, G.L., Cendes, F., Corvin, A., Crespo-Facorro, B., Dalrymple-Alford, J.C., Dannlowski, U., de Geus, E.J.C., Deary, I.J., Delanty, N., Depondt, C., Desrivières, S., Donohoe, G., Espeseth, T., Fernández, G., Fisher, S.E., Flor, H., Forstner, A.J., Francks, C., Franke, B., Glahn, D.C., Gollub, R.L., Grabe, H.J., Gruber, O., Håberg, A.K., Hariri, A.R., Hartman, C.A., Hashimoto, R., Heinz, A., Henskens, F.A., Hillegers, M.H.J., Hoekstra, P.J., Holmes, A.J., Hong, L.E., Hopkins, W.D., Hulshoff Pol, H.E., Jernigan, T.L., Jönsson, E.G., Kahn, R.S., Kennedy, M.A., Kircher, T.T.J., Kochunov, P., Kwok, J.B.J., Le Hellard, S., Loughland, C.M., Martin, N.G., Martinot, J.L., McDonald, C., McMahon, K.L., Meyer-Lindenberg, A., Michie, P.T., Morey, R.A., Mowry, B., Nyberg, L., Oosterlaan, J., Ophoff, R.A., Pantelis, C., Paus, T., Pausova, Z., Penninx, B., Polderman, T.J.C., Posthuma, D., Rietschel, M., Roffman, J.L., Rowland, L.M., Sachdev, P.S., Sämann, P. G., Schall, U., Schumann, G., Scott, R.J., Sim, K., Sisodiya, S.M., Smoller, J.W., Sommer, I.E., St Pourcain, B., Stein, D.J., Toga, A.W., Trollor, J.N., Van der Wee, N.J. A., van 't Ent, D., Völzke, H., Walter, H., Weber, B., Weinberger, D.R., Wright, M.J., Zhou, J., Stein, J.L., Thompson, P.M., Medland, S.E., 2020. The genetic architecture of the human cerebral cortex. Science 367.

Gupta, S., Deshpande, V., 2016. Visual evoked potentials: impact of age, gender, head size and BMI. Int. J. Biomed. Adv. Res. 7, 22.

Himmelberg, M.M., Winawer, J., Carrasco, M., 2022. Linking individual differences in human primary visual cortex to contrast sensitivity around the visual field. Nat. Commun. 13, 3309.

Hinds, O.P., Rajendran, N., Polimeni, J.R., Augustinack, J.C., Wiggins, G., Wald, L.L., Diana Rosas, H., Potthast, A., Schwartz, E.L., Fischl, B., 2008. Accurate prediction of V1 location from cortical folds in a surface coordinate system. Neuroimage 39, 1585–1599.

Hogstrom, L.J., Westlye, L.T., Walhovd, K.B., Fjell, A.M., 2013. The structure of the cerebral cortex across adult life: age-related patterns of surface area, thickness, and gyrification. Cereb. Cortex 23, 2521–2530.

Hyde, K.L., Lerch, J.P., Zatorre, R.J., Griffiths, T.D., Evans, A.C., Peretz, I., 2007. Cortical thickness in congenital amusia: when less is better than more. J. Neurosci. 27, 13028.

Ishibashi, T., Dakin, K.A., Stevens, B., Lee, P.R., Kozlov, S.V., Stewart, C.L., Fields, R.D., 2006. Astrocytes promote myelination in response to electrical impulses. Neuron 49, 823–832.

Jorgensen, K.N., Nerland, S., Norbom, L.B., Doan, N.T., Nesvag, R., Morch-Johnsen, L., Haukvik, U.K., Melle, I., Andreassen, O.A., Westlye, L.T., Agartz, I., 2016. Increased MRI-based cortical grey/white-matter contrast in sensory and motor regions in schizophrenia and bipolar disorder. Psychol. Med. 46, 1971–1985.

Kelly, S., Jahanshad, N., Zalesky, A., Kochunov, P., Agartz, I., Alloza, C., Andreassen, O. A., Arango, C., Banaj, N., Bouix, S., Bousman, C.A., Brouwer, R.M., Bruggemann, J., Bustillo, J., Cahn, W., Calhoun, V., Cannon, D., Carr, V., Catts, S., Chen, J., Chen, J. X., Chen, X., Chiapponi, C., Cho, K.K., Ciullo, V., Corvin, A.S., Crespo-Facorro, B., Cropley, V., De Rossi, P., Diaz-Caneja, C.M., Dickie, E.W., Ehrlich, S., Fan, F.M., Faskowitz, J., Fatouros-Bergman, H., Flyckt, L., Ford, J.M., Fouche, J.P., Fukunaga, M., Gill, M., Glahn, D.C., Gollub, R., Goudzwaard, E.D., Guo, H., Gur, R. E., Gur, R.C., Gurholt, T.P., Hashimoto, R., Hatton, S.N., Henskens, F.A., Hibar, D.P., Hickie, I.B., Hong, L.E., Horacek, J., Howells, F.M., Hulshoff Pol, H.E., Hyde, C.L., Isaev, D., Jablensky, A., Jansen, P.R., Janssen, J., Jonsson, E.G., Jung, L.A., Kahn, R. S., Kikinis, Z., Liu, K., Klauser, P., Knochel, C., Kubicki, M., Lagopoulos, J., Langen, C., Lawrie, S., Lenroot, R.K., Lim, K.O., Lopez-Jaramillo, C., Lyall, A., Magnotta, V., Mandl, R.C.W., Mathalon, D.H., McCarley, R.W., McCarthy-Jones, S., McDonald, C., McEwen, S., McIntosh, A., Melicher, T., Mesholam-Gately, R.I., Michie, P.T., Mowry, B., Mueller, B.A., Newell, D.T., O'Donnell, P., Oertel-Knochel, V., Oestreich, L., Paciga, S.A., Pantelis, C., Pasternak, O., Pearlson, G., Pellicano, G.R., Pereira, A., Pineda Zapata, J., Piras, F., Potkin, S.G., Preda, A., Rasser, P.E., Roalf, D.R., Roiz, R., Roos, A., Rotenberg, D., Satterthwaite, T.D., Savadjiev, P., Schall, U., Scott, R.J., Seal, M.L., Seidman, L.J., Shannon Weickert, C., Whelan, C.D., Shenton, M.E., Kwon, J.S., Spalletta, G., Spaniel, F., Sprooten, E., Stablein, M., Stein, D.J., Sundram, S., Tan, Y., Tan, S., Tang, S., Temmingh, H.S., Westlye, L.T., Tonnesen, S., Tordesillas-Gutierrez, D., Doan, N.T., Vaidya, J., van Haren, N.E.M., Vargas, C.D., Vecchio, D., Velakoulis, D., Voineskos, A., Voyvodic, J. Q., Wang, Z., Wan, P., Wei, D., Weickert, T.W., Whalley, H., White, T., Whitford, T. J., Wojcik, J.D., Xiang, H., Xie, Z., Yamamori, H., Yang, F., Yao, N., Zhang, G., Zhao, J., van Erp, T.G.M., Turner, J., Thompson, P.M., Donohoe, G., 2018. Widespread white matter microstructural differences in schizophrenia across 4322 individuals: results from the ENIGMA Schizophrenia DTI Working Group. Mol. Psychiatry 23, 1261–1269.

Kim, S., Kim, Y.-W., Jeon, H., Im, C.-H., Lee, S.-H., 2020. Altered cortical thickness-based individualized structural covariance networks in patients with schizophrenia and bipolar disorder. J. Clin. Med. 9.

Klein, S.D., Olman, C.A., Sponheim, S.R., 2020. Perceptual mechanisms of visual hallucinations and illusions in psychosis. J. Psychiatr. Brain Sci. 5.

Konopaske, G.T., Lange, N., Coyle, J.T., Benes, F.M., 2014. Prefrontal cortical dendritic spine pathology in schizophrenia and bipolar disorder. JAMA Psychiatry 71, 1323–1331.

Kuperberg, G.R., Broome, M.R., McGuire, P.K., David, A.S., Eddy, M., Ozawa, F., Goff, D., West, W.C., Williams, S.C., van der Kouwe, A.J., Salat, D.H., Dale, A.M., Fischl, B., 2003. Regionally localized thinning of the cerebral cortex in schizophrenia. Arch. Gen. Psychiatry 60, 878–888.

Lalor, E.C., De Sanctis, P., Krakowski, M.I., Foxe, J.J., 2012. Visual sensory processing deficits in schizophrenia: is there anything to the magnocellular account? Schizophr. Res. 139, 246–252.

Lancaster, E., 2016. The diagnosis and treatment of autoimmune encephalitis. J. Clin. Neurol. 12, 1–13.

Lee, W.C., Bonin, V., Reed, M., Graham, B.J., Hood, G., Glattfelder, K., Reid, R.C., 2016. Anatomy and function of an excitatory network in the visual cortex. Nature 532, 370–374.

Liem, F., Zaehle, T., Burkhard, A., Jancke, L., Meyer, M., 2012. Cortical thickness of supratemporal plane predicts auditory N1 amplitude. Neuroreport 23, 1026–1030.

Lim, A., Hoek, H.W., Deen, M.L., Blom, J.D., Bruggeman, R., Cahn, W., de Haan, L., Kahn, R.S., Meijer, C.J., Myin-Germeys, I., van Os, J., Wiersma, D., 2016. Prevalence and classification of hallucinations in multiple sensory modalities in schizophrenia spectrum disorders. Schizophr. Res. 176, 493–499.

Lubiński, W., Grabek-Kujawa, H., Mularczyk, M., Kucharska-Mazur, J., Dańczura, E., Samochowiec, J., 2023. Visual pathway function in untreated individuals with major depression. Adv. Clin. Exp. Med. 32, 117–123.

Luck, S.J., 2014. An Introduction to the Event-Related Potential Technique, 2nd edition. The MIT Press, Cambridge, Massachusetts. ed.

Luck, S.J., Stewart, A.X., Simmons, A.M., Rhemtulla, M., 2021. Standardized measurement error: a universal metric of data quality for averaged event-related potentials. Psychophysiology 58, e13793.

Luders, E., Narr, K.L., Thompson, P.M., Rex, D.E., Woods, R.P., DeLuca, H., Jancke, L., Toga, A.W., 2006. Gender effects on cortical thickness and the influence of scaling. Hum. Brain Mapp. 27, 314–324.

Madre, M., Canales-Rodríguez, E.J., Fuentes-Claramonte, P., Alonso-Lana, S., Salgado-Pineda, P., Guerrero-Pedraza, A., Moro, N., Bosque, C., Gomar, J.J., Ortíz-Gil, J., Goikolea, J.M., Bonnin, C.M., Vieta, E., Sarró, S., Maristany, T., McKenna, P.J., Salvador, R., Pomarol-Clotet, E., 2020. Structural abnormality in schizophrenia versus bipolar disorder: a whole brain cortical thickness, surface area, volume and gyrification analyses. Neuroimage Clin. 25, 102131-102131.

M.D., Ph.D.B.A.M.D. Gluck, Martin R., Thomas, Rohan G., Davis, Kenneth L., Haroutunian, Vahram, 2002. Implications for Altered Glutamate and GABA Metabolism in the Dorsolateral Prefrontal Cortex of Aged Schizophrenic Patients Am. J. Psychiatry 159, 1165–1173.

Mavroudis, I., Petrides, F., Kazis, D., Chatzikonstantinou, S., Karantali, E., Ciobica, A., Iordache, A.-C., Dobrin, R., Trus, C., Njau, S., Costa, V., Baloyannis, S., 2021. Morphological alterations of the pyramidal and stellate cells of the visual cortex in schizophrenia. Exp. Ther. Med. 22, 669-669.

McCarthy, C.S., Ramprashad, A., Thompson, C., Botti, J.A., Coman, I.L., Kates, W.R., 2015. A comparison of FreeSurfer-generated data with and without manual intervention. Front. Neurosci. 9, 379.

McCutcheon, R.A., Keefe, R.S.E., McGuire, P.K., 2023. Cognitive impairment in schizophrenia: aetiology, pathophysiology, and treatment. Mol. Psychiatry.

McGrath, J., Saha, S., Chant, D., Welham, J., 2008. Schizophrenia: a concise overview of incidence, prevalence, and mortality. Epidemiol. Rev. 30, 67–76.

Merikangas, K.R., Jin, R., He, J.-P., Kessler, R.C., Lee, S., Sampson, N.A., Viana, M.C., Andrade, L.H., Hu, C., Karam, E.G., Ladea, M., Medina-Mora, M.E., Ono, Y., Posada-Villa, J., Sagar, R., Wells, J.E., Zarkov, Z., 2011. Prevalence and correlates of bipolar spectrum disorder in the world mental health survey initiativebipolar spectrum in world mental health survey. JAMA Psychiatry 68, 241–251.

Norbom, L.B., Ferschmann, L., Parker, N., Agartz, I., Andreassen, O.A., Paus, T., Westlye, L.T., Tamnes, C.K., 2021. New insights into the dynamic development of the cerebral cortex in childhood and adolescence: integrating macro- and microstructural MRI findings. Prog. Neurobiol., 102109

Normann, C., Schmitz, D., Furmaier, A., Doing, C., Bach, M., 2007a. Long-term plasticity of visually evoked potentials in humans is altered in major depression. Biol. Psychiatry 62, 373–380.
Normann, C., Schmitz, D., Fürmaier, A., Döing, C., Bach, M., 2007b. Long-term plasticity of visually evoked potentials in humans is altered in major depression. Biol. Psychiatry 62, 373–380.
Novitskiy, N., Ramautar, J.R., Vanderperren, K., De Vos, M., Mennes, M., Mijovic, B., Vanrumste, B., Stiers, P., Van den Bergh, B., Lagae, L., Sunaert, S., Van Huffel, S., Wagemans, J., 2011. The BOLD correlates of the visual P1 and N1 in single-trial analysis of simultaneous EEG-fMRI recordings during a spatial detection task. Neuroimage 54, 824–835.
Pajevic, S., Basser, P.J., Fields, R.D., 2014. Role of myelin plasticity in oscillations and synchrony of neuronal activity. Neuroscience 276, 135–147.
Panizzon, M.S., Fennema-Notestine, C., Eyler, L.T., Jernigan, T.L., Prom-Wormley, E., Neale, M., Jacobson, K., Lyons, M.J., Grant, M.D., Franz, C.E., Xian, H., Tsuang, M., Fischl, B., Seidman, L., Dale, A., Kremen, W.S., 2009. Distinct genetic influences on cortical surface area and cortical thickness. Cerebral cortex (New York, N.Y.: 1991) 19, 2728–2735.
Paolicelli, R.C., Bolasco, G., Pagani, F., Maggi, L., Scianni, M., Panzanelli, P., Giustetto, M., Ferreira, T.A., Guiducci, E., Dumas, L., Ragozzino, D., Gross, C.T., 2011. Synaptic pruning by microglia is necessary for normal brain development. Science 333, 1456–1458.
Pieters, L.E., Nadesalingam, N., Walther, S., van Harten, P.N., 2022. A systematic review of the prognostic value of motor abnormalities on clinical outcome in psychosis. Neurosci. Biobehav. Rev. 132, 691–705.
Pontious, A., Kowalczyk, T., Englund, C., Hevner, R.F., 2008. Role of intermediate progenitor cells in cerebral cortex development. Dev. Neurosci. 30, 24–32.
Rakic, P., 1995. A small step for the cell, a giant leap for mankind: a hypothesis of neocortical expansion during evolution. Trends Neurosci. 18, 383–388.
Reavis, E.A., Lee, J., Altshuler, L.L., Cohen, M.S., Engel, S.A., Glahn, D.C., Jimenez, A.M., Narr, K.L., Nuechterlein, K.H., Riedel, P., Wynn, J.K., Green, M.F., 2020. Structural and functional connectivity of visual cortex in schizophrenia and bipolar disorder: a graph-theoretic analysis. Schizophrenia Bull. Open 1, sgaa056.
Reavis, E.A., Lee, J., Wynn, J.K., Engel, S.A., Jimenez, A.M., Green, M.F., 2017a. Cortical thickness of functionally defined visual areas in schizophrenia and bipolar disorder. Cereb. Cortex 27, 2984–2993.
Reavis, E.A., Lee, J., Wynn, J.K., Narr, K.L., Njau, S.N., Engel, S.A., Green, M.F., 2017b. Linking optic radiation volume to visual perception in schizophrenia and bipolar disorder. Schizophr. Res. 190, 102–106.
Rimol, L.M., Nesvåg, R., Hagler, D.J., Bergmann, Ø., Fennema-Notestine, C., Hartberg, C. B., Haukvik, U.K., Lange, E., Pung, C.J., Server, A., Melle, I., Andreassen, O.A., Agartz, I., Dale, A.M., 2012. Cortical Volume, Surface Area, and Thickness in Schizophrenia and Bipolar Disorder. Biol. Psychiatry 71, 552–560.
Ritchie, S.J., Cox, S.R., Shen, X., Lombardo, M.V., Reus, L.M., Alloza, C., Harris, M.A., Alderson, H.L., Hunter, S., Neilson, E., Liewald, D.C.M., Auyeung, B., Whalley, H.C., Lawrie, S.M., Gale, C.R., Bastin, M.E., McIntosh, A.M., Deary, I.J., 2018. Sex Differences in the adult human brain: evidence from 5216 UK biobank participants. Cereb. Cortex 28, 2959–2975.
Romanos, J., Benke, D., Saab, A.S., Zeilhofer, H.U., Santello, M., 2019. Differences in glutamate uptake between cortical regions impact neuronal NMDA receptor activation. Commun. Biol. 2, 127.
Rosen, A.F.G., Roalf, D.R., Ruparel, K., Blake, J., Seelaus, K., Villa, L.P., Ciric, R., Cook, P. A., Davatzikos, C., Elliott, M.A., Garcia de La Garza, A., Gennatas, E.D., Quarmley, M., Schmitt, J.E., Shinohara, R.T., Tisdall, M.D., Craddock, R.C., Gur, R. E., Gur, R.C., Satterthwaite, T.D., 2018. Quantitative assessment of structural image quality. Neuroimage 169, 407–418.
Sarnthein, J., Andersson, M., Zimmermann, M.B., Zumsteg, D., 2009. High test-retest reliability of checkerboard reversal visual evoked potentials (VEP) over 8 months. Clin. Neurophysiol. 120, 1835–1840.
Schwarzkopf, D.S., Robertson, D.J., Song, C., Barnes, G.R., Rees, G., 2012. The frequency of visually induced γ-band oscillations depends on the size of early human visual cortex. J. Neurosci. 32, 1507–1512.
Sellgren, C.M., Gracias, J., Watmuff, B., Biag, J.D., Thanos, J.M., Whittredge, P.B., Fu, T., Worringer, K., Brown, H.E., Wang, J., Kaykas, A., Karmacharya, R., Goold, C.P., Sheridan, S.D., Perlis, R.H., 2019. Increased synapse elimination by microglia in schizophrenia patient-derived models of synaptic pruning. Nat. Neurosci. 22, 374–385.
Sharma, R., Joshi, S., Singh, K.D., Kumar, A., 2015. Visual evoked potentials: normative values and gender differences. J. Clin. Diagn. Res. 9, CC12–CC15.
Shigihara, Y., Hoshi, H., Zeki, S., 2016. Early visual cortical responses produced by checkerboard pattern stimulation. Neuroimage 134, 532–539.
Song, C., Schwarzkopf, D.S., Kanai, R., Rees, G., 2015. Neural population tuning links visual cortical anatomy to human visual perception. Neuron 85, 641–656.
Spencer, K.M., Nestor, P.G., Niznikiewicz, M.A., Salisbury, D.F., Shenton, M.E., McCarley, R.W., 2003. Abnormal neural synchrony in schizophrenia. J. Neurosci. 23, 7407.
Strike, L.T., Hansell, N.K., Couvy-Duchesne, B., Thompson, P.M., de Zubicaray, G.I., McMahon, K.L., Wright, M.J., 2019. Genetic complexity of cortical structure: differences in genetic and environmental factors influencing cortical surface area and thickness. Cereb. Cortex 29, 952–962.
Takahashi, N., Sakurai, T., Davis, K.L., Buxbaum, J.D., 2011. Linking oligodendrocyte and myelin dysfunction to neurocircuitry abnormalities in schizophrenia. Prog. Neurobiol. 93, 13–24.
Thalheimer, W., Cook, S., 2009. How to calculate effect sizes from published research: a simplified methodology.
Uhlhaas, P.J., Singer, W., 2006. Neural synchrony in brain disorders: relevance for cognitive dysfunctions and pathophysiology. Neuron 52, 155–168.
Valstad, M., Moberget, T., Roelfs, D., Slapø, N.B., Timpe, C.M.F., Beck, D., Richard, G., Sæther, L.S., Haatveit, B., Skaug, K.A., Nordvik, J.E., Hatlestad-Hall, C., Einevoll, G. T., Mäki-Marttunen, T., Westlye, L.T., Jönsson, E.G., Andreassen, O.A., Elvsåshagen, T., 2020. Experience-dependent modulation of the visual evoked potential: testing effect sizes, retention over time, and associations with age in 415 healthy individuals. Neuroimage 223, 117302.
Valstad, M., Roelfs, D., Slapo, N.B., Timpe, C.M.F., Rai, A., Matziorinis, A.M., Beck, D., Richard, G., Saether, L.S., Haatveit, B., Nordvik, J.E., Hatlestad-Hall, C., Einevoll, G. T., Maki-Marttunen, T., Haram, M., Ueland, T., Lagerberg, T.V., Steen, N.E., Melle, I., Westlye, L.T., Jonsson, E.G., Andreassen, O.A., Moberget, T., Elvsashagen, T., 2021. Evidence for reduced long-term potentiation-like visual cortical plasticity in schizophrenia and bipolar disorder. Schizophr. Bull.
van Erp, T.G.M., Walton, E., Hibar, D.P., Schmaal, L., Jiang, W., Glahn, D.C., Pearlson, G. D., Yao, N., Fukunaga, M., Hashimoto, R., Okada, N., Yamamori, H., Bustillo, J.R., Clark, V.P., Agartz, I., Mueller, B.A., Cahn, W., de Zwarte, S.M.C., Hulshoff Pol, H.E., Kahn, R.S., Ophoff, R.A., van Haren, N.E.M., Andreassen, O.A., Dale, A.M., Doan, N. T., Gurholt, T.P., Hartberg, C.B., Haukvik, U.K., Jorgensen, K.N., Lagerberg, T.V., Melle, I., Westlye, L.T., Gruber, O., Kraemer, B., Richter, A., Zilles, D., Calhoun, V.D., Crespo-Facorro, B., Roiz-Santianez, R., Tordesillas-Gutierrez, D., Loughland, C., Carr, V.J., Catts, S., Cropley, V.L., Fullerton, J.M., Green, M.J., Henskens, F.A., Jablensky, A., Lenroot, R.K., Mowry, B.J., Michie, P.T., Pantelis, C., Quide, Y., Schall, U., Scott, R.J., Cairns, M.J., Seal, M., Tooney, P.A., Rasser, P.E., Cooper, G., Shannon Weickert, C., Weickert, T.W., Morris, D.W., Hong, E., Kochunov, P., Beard, L.M., Gur, R.E., Gur, R.C., Satterthwaite, T.D., Wolf, D.H., Belger, A., Brown, G.G., Ford, J.M., Macciardi, F., Mathalon, D.H., O'Leary, D.S., Potkin, S.G., Preda, A., Voyvodic, J., Lim, K.O., McEwen, S., Yang, F., Tan, Y., Tan, S., Wang, Z., Fan, F., Chen, J., Xiang, H., Tang, S., Guo, H., Wan, P., Wei, D., Bockholt, H.J., Ehrlich, S., Wolthusen, R.P.F., King, M.D., Shoemaker, J.M., Sponheim, S.R., De Haan, L., Koenders, L., Machielsen, M.W., van Amelsvoort, T., Veltman, D.J., Assogna, F., Banaj, N., de Rossi, P., Iorio, M., Piras, F., Spalletta, G., McKenna, P.J., Pomarol-Clotet, E., Salvador, R., Corvin, A., Donohoe, G., Kelly, S., Whelan, C.D., Dickie, E.W., Rotenberg, D., Voineskos, A.N., Ciufolini, S., Radua, J., Dazzan, P., Murray, R., Reis Marques, T., Simmons, A., Borgwardt, S., Egloff, L., Harrisberger, F., Riecher-Rossler, A., Smieskova, R., Alpert, K.I., Wang, L., Jonsson, E.G., Koops, S., Sommer, I.E.C., Bertolino, A., Bonvino, A., Di Giorgio, A., Neilson, E., Mayer, A.R., Stephen, J.M., Kwon, J.S., Yun, J.Y., Cannon, D.M., McDonald, C., Lebedeva, I., Tomyshev, A.S., Akhadov, T., Kaleda, V., Fatouros-Bergman, H., Flyckt, L., Karolinska Schizophrenia, P., Busatto, G.F., Rosa, P.G.P., Serpa, M.H., Zanetti, M.V., Hoschl, C., Skoch, A., Spaniel, F., Tomecek, D., Hagenaars, S.P., McIntosh, A.M., Whalley, H.C., Lawrie, S.M., Knochel, C., Oertel-Knochel, V., Stablein, M., Howells, F.M., Stein, D.J., Temmingh, H.S., Uhlmann, A., Lopez-Jaramillo, C., Dima, D., McMahon, A., Faskowitz, J.I., Gutman, B.A., Jahanshad, N., Thompson, P. M., Turner, J.A., 2018. Cortical brain abnormalities in 4474 individuals with schizophrenia and 5098 control subjects via the enhancing neuro imaging genetics through meta analysis (ENIGMA) consortium. Biol. Psychiatry 84, 644–654.
Waters, F., Collerton, D., Ffytche, D.H., Jardri, R., Pins, D., Dudley, R., Blom, J.D., Mosimann, U.P., Eperjesi, F., Ford, S., Laroi, F., 2014. Visual hallucinations in the psychosis spectrum and comparative information from neurodegenerative disorders and eye disease. Schizophr. Bull. 40 (Suppl 4), S233–S245.
Whittingstall, K., Stroink, G., Schmidt, M., 2007. Evaluating the spatial relationship of event-related potential and functional MRI sources in the primary visual cortex. Hum. Brain Mapp. 28, 134–142.
Wickham, H., 2016. Data Analysis. In: Wickham, H. (Ed.), ggplot2: Elegant Graphics for Data Analysis. Springer International Publishing, Cham, pp. 189–201.
Wierenga, L.M., Langen, M., Oranje, B., Durston, S., 2014. Unique developmental trajectories of cortical thickness and surface area. Neuroimage 87, 120–126.
Winkler, A.M., Kochunov, P., Blangero, J., Almasy, L., Zilles, K., Fox, P.T., Duggirala, R., Glahn, D.C., 2010. Cortical thickness or grey matter volume? The importance of selecting the phenotype for imaging genetics studies. Neuroimage 53, 1135–1146.
Yeap, S., Kelly, S.P., Sehatpour, P., Magno, E., Garavan, H., Thakore, J.H., Foxe, J.J., 2008. Visual sensory processing deficits in Schizophrenia and their relationship to disease state. Eur. Arch. Psychiatry Clin. Neurosci. 258, 305–316.
Yeap, S., Kelly, S.P., Sehatpour, P., Magno, E., Javitt, D.C., Garavan, H., Thakore, J.H., Foxe, J.J., 2006. Early visual sensory deficits as endophenotypes for schizophrenia: high-density electrical mapping in clinically unaffected first-degree relatives. Arch. Gen. Psychiatry 63, 1180–1188.
Yoon, J.H., Maddock, R.J., Rokem, A., Silver, M.A., Minzenberg, M.J., Ragland, J.D., Carter, C.S., 2010. GABA concentration is reduced in visual cortex in schizophrenia and correlates with orientation-specific surround suppression. J. Neurosci. 30, 3777–3781.
Zak, N., Moberget, T., Bøen, E., Boye, B., Waage, T.R., Dietrichs, E., Harkestad, N., Malt, U.F., Westlye, L.T., Andreassen, O.A., Andersson, S., Elvsåshagen, T., 2018. Longitudinal and cross-sectional investigations of long-term potentiation-like cortical plasticity in bipolar disorder type II and healthy individuals. Transl. Psychiatry 8, 103.
Zalc, B., Fields, R.D., 2000. Do action potentials regulate myelination? Neuroscientist 6, 5–13.
Zhu, Z., Zhao, Y., Wen, K., Li, Q., Pan, N., Fu, S., Li, F., Radua, J., Vieta, E., Kemp, G.J., Biswa, B.B., Gong, Q., 2022. Cortical thickness abnormalities in patients with bipolar disorder: a systematic review and meta-analysis. J. Affect. Disord. 300, 209–218.